VIP Oxygen Reduction Very Important Paper

International Edition: DOI: 10.1002/anie.201503159
German Edition: DOI: 10.1002/ange.201503159

S-Doping of an Fe/N/C ORR Catalyst for Polymer Electrolyte Membrane Fuel Cells with High Power Density**

Yu-Cheng Wang, Yu-Jiao Lai, Lin Song, Zhi-You Zhou, Jian-Guo Liu, Qiang Wang, Xiao-Dong Yang, Chi Chen, Wei Shi, Yan-Ping Zheng, Muhammad Rauf, and Shi-Gang Sun**

Abstract: *Fe/N/C is a promising non-Pt electrocatalyst for the oxygen reduction reaction (ORR), but its catalytic activity is considerably inferior to that of Pt in acidic medium, the environment of polymer electrolyte membrane fuel cells (PEMFCs). An improved Fe/N/C catalyst (denoted as Fe/N/C-SCN) derived from $Fe(SCN)_3$, poly-m-phenylenediamine, and carbon black is presented. The advantage of using $Fe(SCN)_3$ as iron source is that the obtained catalyst has a high level of S doping and high surface area, and thus exhibits excellent ORR activity ($23\ A\,g^{-1}$ at 0.80 V) in 0.1 M H_2SO_4 solution. When the Fe/N/C-SCN was applied in a PEMFC as cathode catalyst, the maximal power density could exceed $1\ W\,cm^{-2}$.*

The bottleneck of polymer electrolyte membrane fuel cells (PEMFCs) is high cost, since expensive Pt catalysts are necessary to drive both the cathodic oxygen reduction reaction (ORR) and anodic hydrogen oxidation.[1] The ORR is kinetically very slow, and requires much more Pt catalyst than hydrogen oxidation. Therefore, the exploration of non-Pt catalysts for the ORR has received great interest. Ternary Fe/N/C is generally considered as one of the most promising candidates.[2] The development of Fe/N/C catalyst can be traced back to the pioneering work of transition-metal macrocyclic compounds by Jasinski.[3] Currently, macrocyclic compounds are unnecessary, because high-temperature pyrolysis of a mixture of iron salts, nitrogen-containing species, and carbon support can also yield such a catalyst even with better activity and stability.[2a,b,4] Fe/N/C catalysts can exhibit an ORR activity in both acidic and alkaline solutions. However, the former is more challenging and important in consideration of the strong acidic and corrosive environment of Nafion-based PEMFCs.[5]

Significant progress has been achieved in synthesis of highly active Fe/N/C catalyst and exploration of their applications in PEMFCs recently.[6] For example, Dodelet et al. found that ball-milling precursors and two-step pyrolysis in an Ar and NH_3 atmosphere can greatly boost the ORR activity of Fe/N/C catalyst, yielding a maximal power density (P_{max}) of $0.45\ W\,cm^{-2}$ in PEMFC test.[2a] They further improved the P_{max} to $0.91\ W\,cm^{-2}$ at 1 bar back-pressure using a high-surface-area metal–organic framework as support.[7] Liu et al. reported the synthesis of polyporphyrin-based Fe/N/C catalysts with a P_{max} of about $0.73\ W\,cm^{-2}$.[8] Alternatively, Zelenay and co-workers reported an Fe/N/C derived from polyaniline, carbon black, and $FeCl_3$ through a procedure of pyrolysis, acid leaching, and secondary pyrolysis. The obtained Fe/N/C catalyst exhibited a high ORR activity (ca. $6.7\ A\,g^{-1}$ at 0.80 V) and an extremely low H_2O_2 yield (< 1%) in rotating ring-disk electrode (RRDE) test, and a P_{max} of $0.55\ W\,cm^{-2}$ at 1.8 bar back-pressure in a PEMFC test.[2b] Nevertheless, both ORR activity and PEMFC performance of Fe/N/C catalysts still need further improvement for practical applications.

We previously prepared a highly active Fe/N/C catalyst ($11.5\ A\,g^{-1}$ at 0.80 V) from nitrogen-abundant poly-*m*-phenylenediamine (P*m*PDA) and $FeCl_3$,[9] according to the revised Zelenay method.[2b] The P_{max} was $0.35\ W\,cm^{-2}$ without back-pressure in a preliminary fuel cell test. Herein we find that iron salts can also greatly influence the ORR activity of Fe/N/C, and the use of $Fe(SCN)_3$ instead of $FeCl_3$ can nearly double the ORR activity. The improvement may be correlated with S doping and high surface area. The P_{max} of PEMFC using this improved catalyst reached 0.94 and $1.03\ W\,cm^{-2}$ at 1 and 2 bar back-pressure, respectively.

The synthesis of P*m*PDA-based catalyst was similar to that reported previously.[9] In brief, P*m*PDA was coated onto sulfophenyl-grafted carbon black through oxidative polymerization of *m*-PDA monomer by $(NH_4)_2S_2O_8$. After adding $FeCl_3$ or $Fe(SCN)_3$, the precursor was subjected sequentially to pyrolysis at 950 °C under Ar atmosphere, acid leaching, and secondary pyrolysis. Catalysts prepared using $FeCl_3$ and $Fe(SCN)_3$ are denoted as Fe/N/C-Cl and Fe/N/C-SCN, respectively. High-resolution transmission electron microsco-

[*] Y. C. Wang, Y. J. Lai, L. Song, Prof. Z. Y. Zhou, Dr. Q. Wang, Dr. X. D. Yang, C. Chen, W. Shi, Y. P. Zheng, M. Rauf, Prof. S. G. Sun
State Key Laboratory of Physical Chemistry of Solid Surfaces
Collaborative innovation center of Chemistry for Energy Materials
College of Chemistry and Chemical Engineering
Xiamen University, Xiamen, 361005 (China)
E-mail: zhouzy@xmu.edu.cn
sgsun@xmu.edu.cn
Prof. J. G. Liu
Eco-materials and Renewable Energy Research Center
Department of Materials Science and Engineering
and National Laboratory of Solid State Microstructures
Nanjing University, Nanjing 210093 (China)
C. Chen
State Key Laboratory of Chemical Engineering
College of Chemical Engineering
East China University of Science and Technology
Shanghai, 200237 (China)

[**] This study was supported by grants from Major State Basic Research Development Program of China (2015CB932300), NSFC (21373175, 21321062 and 21361140374), Program for New Century Excellent Talents in University (NECT-11-0301). ORR = oxygen reduction reaction.

Supporting information for this article is available on the WWW under http://dx.doi.org/10.1002/anie.201503159.

py (HRTEM) measurements indicate that the Fe/N/C-SCN consists of carbon nanoparticles of 100–200 nm in size, and no crystalline metal-containing phases (for example, Fe, FeS, and Fe_3C), which should display high contrast in TEM images, could be observed (Supporting Information, Figure S1).

Figure 1 a compares ORR polarization curves of Fe/N/C-SCN, Fe/N/C-Cl, and commercial Pt/C (20 wt%; JM) catalysts in O_2-saturated 0.1 M H_2SO_4 solution. Catalyst loading was 0.6 mg cm^{-2} for Fe/N/C catalysts and 0.1 mg cm^{-2} (or 20 μg_{Pt} cm^{-2}) for Pt/C. The catalytic activity of Fe/N/C-SCN is considerably higher than that of Fe/N/C-Cl, as evidenced by higher (0.836 vs. 0.820 V) half-wave potential ($E_{1/2}$). The $E_{1/2}$ of Fe/N/C-SCN was only 48 mV lower than that of Pt/C.

To quantitatively compare the intrinsic activity, kinetic current was calculated through Koutecky–Levich equation, and was then normalized with catalyst loading to obtain mass activity (j_m). Figure 1 b illustrates Tafel plots of the above three catalysts. All catalyst yielded a similar Tafel slope, that is, 66, 64, and 69 mV, for Fe/N/C-SCN, Fe/N/C-Cl, and Pt/C, respectively. The measured mass activities of Fe/N/C-SCN and Fe/N/C-Cl were 23.0 and 13.4 A g^{-1} at 0.80 V (inset of Figure 1 b), as well as 0.75 and 0.35 A g^{-1} at 0.90 V, respectively. Clearly, the use of $Fe(SCN)_3$ instead of $FeCl_3$ as Fe source can improve significantly the ORR activity, although H_2O_2 yield increased slightly (1.5% vs. 1.0% at 0.70 V, Figure 1 a). Note that the catalytic activity of Fe/N/C-Cl is slightly higher than that reported previously,[9] since the amount of $FeCl_3$ was further optimized during the preparation of the catalyst in this study. As for Pt/C, mass activity at 0.90 V was 23 A $g_{cat.}^{-1}$ (or 115 A g_{Pt}^{-1}). Thus, the mass activity of Fe/N/C-SCN reached to about 1/30 that of Pt/C (20 wt%).

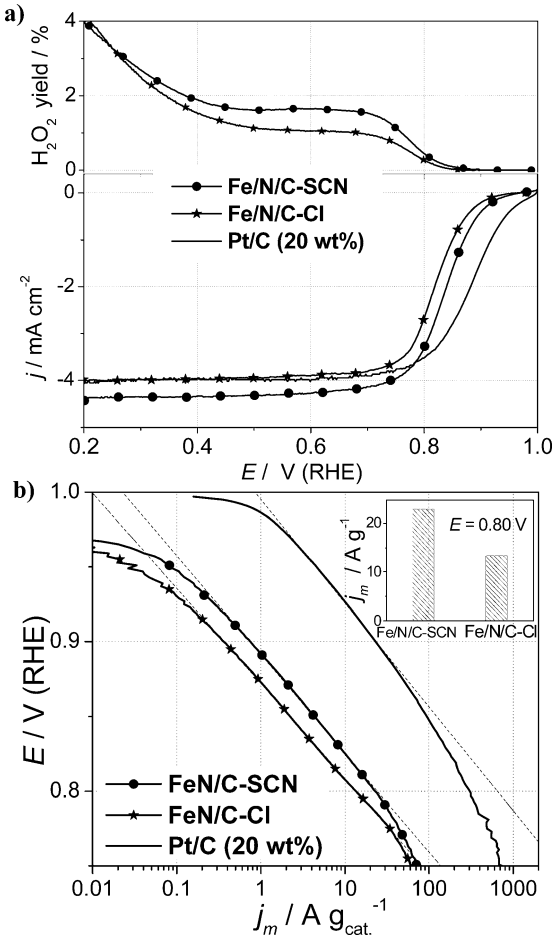

Figure 1. a) ORR polarization curves and H_2O_2 yield of Fe/N/C-SCN, Fe/N/C-Cl, and Pt/C in O_2-saturated 0.1 M H_2SO_4 solution. Rotating speed: 900 rpm; scan rate: 10 mV s^{-1}; Fe/N/C catalyst loading: 0.6 mg cm^{-2}; Pt/C loading: 0.1 mg cm^{-2} (or 20 μg_{Pt} cm^{-2}); 30 °C water bath. b) Tafel plot. Inset: comparison of kinetic current at 0.80 V between Fe/N/C-SCN and Fe/N/C-Cl.

Furthermore, we carried out an H_2–O_2 PEMFC test. Membrane electrode assemblies (MEAs) consisted of Fe/N/C (4.0 mg cm^{-2}) as cathode catalyst for ORR, and Pt/C (0.4 mg_{Pt} cm^{-2}) as anode catalyst for H_2 oxidation. To enhance mass transfer, a back-pressure of 1 or 2 bar was applied (absolute pressure of H_2 or O_2 was about 1.5 or 2.5 bar, respectively, considering 0.47 bar of water saturation vapor pressure at 80 °C). Figure 2 illustrates the polarization curves

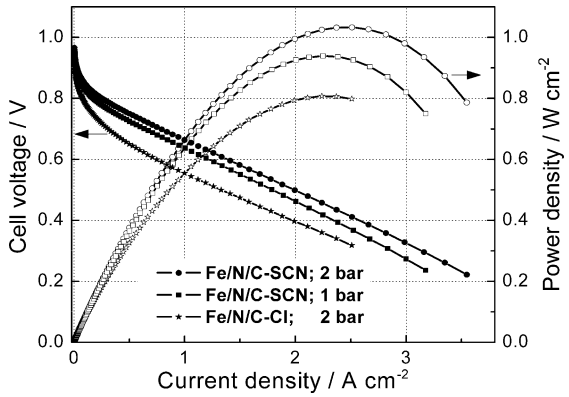

Figure 2. Polarization (left, filled symbols) and power density (right, open symbols) plots for H_2-O_2 PEMFC with Fe/N/C-SCN and Fe/N/C-Cl as cathode catalysts at 80 °C. The back-pressure was 2 or 1 bar as indicated; flow rate: 0.3 slpm; MEA active area: 1.0 cm^2; NRE 211 membrane; cathode catalyst loading: 4.0 mg cm^{-2}; anode catalyst: Pt/C (40 wt%, JM) with 0.4 mg_{Pt} cm^{-2}.

and power-density plots of the PEMFC with Fe/N/C-SCN as cathode catalyst. At 2 bar back-pressure, P_{max} could reach a value as high as 1.03 W cm^{-2} at 0.41 V, and the maximal current density was 3.55 A cm^{-2} at 0.22 V. Decreasing the back-pressure to 1 bar, P_{max} was still 0.94 W cm^{-2}. To the best of our knowledge, this is the highest P_{max} reported so far for PEMFCs with Fe/N/C as cathode catalyst (Supporting Information, Table S1). The area-specific ohmic resistance of MEAs varied within 60–80 mΩ cm^2 during a fuel-cell test. After *iR* correction, Tafel plots (Supporting Information, Figure S2) were obtained. The Tafel slope based on fuel cell data is 80–84 mV, which was higher than the value of 66 mV based on RRDE data. This difference may be attributed to different test temperatures (80 °C vs. 30 °C) and electrolytes (Nafion ionomer vs. 0.1 M H_2SO_4). The observed and *iR*-free current densities at 0.80 V were 0.25 and 0.38 A cm^{-2}, respectively, at 2 bar back-pressure. For Fe/N/C-Cl, P_{max} was only 0.81 W cm^{-2} at 2 bar back-pressure, which was considerably lower than that of Fe/N/C-SCN. Note that the fuel cell

performance of Fe/N/C-Cl is significantly higher than that we reported previously,[9] as we have optimized the fabrication method for MEAs and improved the mass transfer greatly.

For comparison, we also tested the performance of a fuel cell using commercial Pt/C ($0.2\,mg\,Pt\,cm^{-2}$) as cathode catalyst at 1 bar back-pressure (Supporting Information, Figure S3). At a current density below $1\,A\,cm^{-2}$, the performance of the fuel cell using Fe/N/C-SCN is close to that using Pt/C as cathode catalyst. However, at higher current density ($>1\,A\,cm^{-2}$) where mass transfer overweighs electrochemical kinetics, the Pt/C exhibits a performance much better ($P_{max} = 1.77\,W\,cm^{-2}$) than the Fe/N/C-SCN owing to fast mass transfer of the thin Pt/C catalyst layer (ca. 10 μm). How to fabricate thick Fe/N/C catalyst layer (ca. 100 μm) with fast mass transfer would be the key issue in further study.

Apart from activity, the durability of Fe/N/C is also important for fuel-cell applications. To evaluate the durability, the PEMFC with Fe/N/C-SCN catalyst was operated at 0.50 V for 100 h. The current density decreased from 1.60 to $0.77\,A\,cm^{-2}$ in the initial 10 h, and then gradually declined to $0.45\,A\,cm^{-2}$ at 100 h (Supporting Information, Figure S4). Water flooding has been considered as a reason for instability.[10] However, we found that adding some waterproof reagents (for example, dimethyl silicone oil[11]) could not improve the durability (Supporting Information, Figure S4). Further work is therefore still required to improve durability.

To understand why Fe/N/C catalyst prepared from Fe-$(SCN)_3$ has better ORR catalytic activity than that from $FeCl_3$, we carried out some physical characterizations. Figure 3 compares X-ray photoelectron spectroscopy (XPS) of Fe/N/C-SCN and Fe/N/C-Cl. Both catalysts contained C, N, Fe, S, and O elements. According to the relative sensitivity factor method,[12] weight contents of N, Fe, and S were determined to be 4.4%, 1.4%, and 2.1% for Fe/N/C-SCN, as well as 4.9%, 2.2%, and 0.7% for Fe/N/C-Cl, respectively. In another words, Fe/N/C-SCN contained slightly less N and Fe but three times more S in comparison with Fe/N/C-Cl. High-resolution spectra of N_{1s} and Fe_{2p} are similar for both catalysts (inset of Figure 3), therefore, the higher ORR catalytic activity of the Fe/N/C-SCN than Fe/N/C-Cl may be correlated with more S doping. As reported previously, the doping of S in graphene can change electric structure, which benefits ORR.[13]

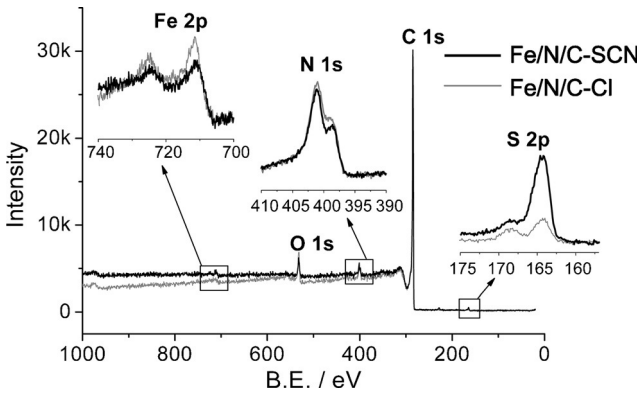

Figure 3. XPS of Fe/N/C-SCN (black line) and Fe/N/C-Cl (gray line). Inset: High-resolution spectra of S 2p, N 1s, and Fe 2p.

Along with S doping, a high specific surface area also contributes to high catalytic activity. Figure 4 demonstrates Ar adsorption–desorption isotherms of Fe/N/C-SCN and Fe/N/C-Cl. The Brunauer–Emmett–Teller (BET) surface area of Fe/N/C-SCN is $751\,m^2\,g^{-1}$, which is significantly larger than

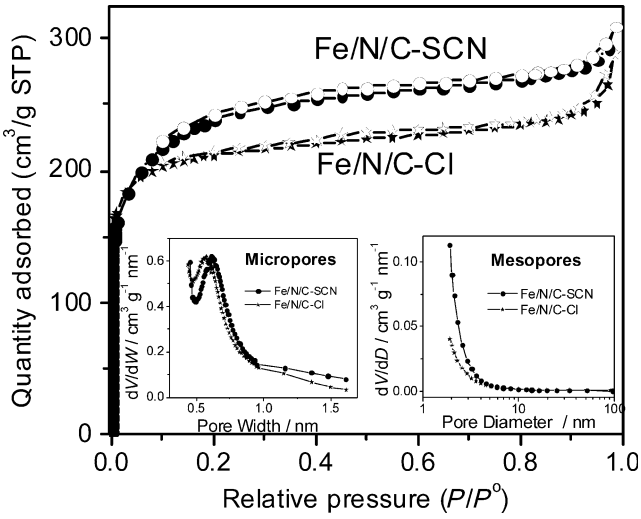

Figure 4. Ar adsorption/desorption isotherm of Fe/N/C-SCN and Fe/N/C-Cl. Filled symbols: adsorption; hollow symbols: desorption. Inset: micropore (HK method) and mesopore (BJH method) size distributions.

$751\,m^2\,g^{-1}$, which is significantly larger than that of Fe/N/C-Cl ($656\,m^2\,g^{-1}$). Results of *t*-plot analysis show that Fe/N/C-SCN has much larger external surface area (337 vs. $158\,m^2\,g^{-1}$) but smaller micropore area (414 vs. $498\,m^2\,g^{-1}$) than Fe/N/C-Cl. The pore-size distribution was analyzed by the Horvath–Kawazoe (HK) method for micropores (<2 nm) and the Barret–Joyner–Halenda (BJH) method for mesopores (>2 nm) (inset to Figure 4). Clearly, Fe/N/C-SCN has more pores of 1.0–4.0 nm than Fe/N/C-Cl, bur less micropores of size below 0.6 nm. In the fuel-cell test, the high external surface area and large pore size of the Fe/N/C-SCN can facilitate the accessibility of reactant for ORR.

As for the Fe/N/C, the catalytic activity depends on turnover frequency (TOF), the density of active sites ($d_{active\,site}$), and surface area (that is, $Activity \propto TOF \times d_{active\,site} \times Area$). When the RDE catalytic activity at 0.80 V was normalized by surface area, Fe/N/C-SCN has higher catalytic activity per BET area (0.031 vs. $0.020\,A\,m^{-2}$) and per micropore area (0.056 vs. $0.027\,A\,m^{-2}$) than Fe/N/C-Cl, but slight lower catalytic activity per external surface area than Fe/N/C-Cl (0.068 vs. $0.084\,A\,m^{-2}$). The S-doping of Fe/N/C-SCN may increase the TOF. Unfortunately, we do not know the density of active sites and where the active sites mainly locate (micropore, or external surface area, or both), so the TOF of the catalysts could not be evaluated experimentally.

In summary, we found that iron salts can greatly influence the ORR performance of pyrolyzed Fe/N/C catalyst, and $Fe(SCN)_3$ can result in S-doping catalyst with high surface area, thereby leading to high ORR activity. The maximal

power density of PEMFC using as-prepared Fe/N/C-SCN can reach as high as 1.03 W cm^{-2}, demonstrating its promising application in PEMFCs.

Experimental Section

The catalysts were prepared according to a previous method.[9] In brief, KJ600 carbon black (2 g) was grafted with sulfophenyl group through reduction of diazonium salt by Fe power. The grafted carbon black was mixed with *m*-phenylenediamine (*m*-PDA, 15 g) and concentrated HCl (36%, 50 mL). To oxidatively polymerize *m*-PDA, $(NH_4)_2S_2O_8$ (2 M, 140 mL) and $FeCl_3$ solution (1 M, 40 mL) were added dropwise. The suspension was filtered and washed to remove inorganic salts including Fe salt. To synthesize Fe/N/C-SCN, the obtained powder (0.3 g) was added into $Fe(SCN)_3$ solution that was prepared by mixing $FeCl_3$ (1 M, 0.9 mL) with KSCN (1 M, 3 mL). The solvent was then removed and further dried at 80 °C for 12 h. The resulting powder was pyrolyzed at 950 °C in an Ar atmosphere for 1 h. The pyrolyzed sample was subjected to acid leaching in 1 M HCl solution at 80 °C for 8 h followed by centrifugation and water washing. Finally, the obtained powder was further pyrolyzed at 950 °C for 3 h to obtain the final catalyst.

The ORR performance was tested in O_2-saturated 0.1 M H_2SO_4 solution at 30 °C on a rotating ring-disk electrode (RRDE) system (Pine Inc.) with a CHI-760D bipotentiostat. Rotating rate was 900 rpm. A glassy carbon (GC, $\phi = 5.61$ mm) disk-Pt ring RRDE was used. A GC plate and a reversible hydrogen electrode (RHE) were used as counter electrode and reference electrode, respectively. To prepare catalyst ink, the Fe/N/C catalyst (6.0 mg) was ultrasonically dispersed in a mixture of water (0.50 mL), ethanol (0.50 mL) and 5% Nafion (0.05 mL) for 1 h. The 25 μL of ink was pipetted onto the GC disk electrode, resulting in catalyst loading of 0.6 mg cm^{-2}. The loading of Pt/C (20 wt%) catalyst was 0.1 mg cm^{-2}. Polarization curves were recorded by potential cycling between 0.2 and 1.0 V at 10 mV s^{-1}. Solution ohmic drop (that is, *iR* drop) was compensated. Capacitive background current was corrected by subtracting the curve recorded in N_2-saturated solution. To determine H_2O_2 yield, the ring electrode was held at 1.30 V to oxidize H_2O_2 diffused from disk electrode.

Membrane electrode assembly (MEA) was prepared through hot-pressing method. The catalyst "ink" was prepared by ultrasonic dispersion of Fe/N/C catalyst (26 mg) and 5 wt% Nafion solution (600 μL) into 1.0 mL deionied water for 1 hour. The ink was directly coated on PTFE-pretreated Toray 060 carbon paper as cathode, and no microporous layer was used. The loading of Fe/N/C catalysts was 4.0 mg cm^{-2}. The Nafion content in the cathode catalyst layer was about 50 wt%. The anode catalyst is 40 wt% Pt/C with a loading of 0.4 mg Pt cm^{-2}. Note that higher Pt content catalyst was used in the fuel cell test than in the RDE test, because it can result in thinner catalyst layer that benefits the mass transfer. Then, the MEA was prepared by hot-pressing cathode, anode, NRE 211 Nafion membrane, and gasket at about 3 MPa for 135 s. The compression was 15–20%. The thickness of cathode catalyst layer was about 100 μm. The active area of MEA was 1.0×1.0 cm^2. Fuel cell performance was tested at 80 °C on Model 850e fuel cell test system (Scribner Associates Inc.). H_2 and O_2 flow rates were 0.3 slpm at 100% RH for polarization curve measurement, and 0.2 slpm for durability test. A back-pressure of 1 or 2 bar was applied.

XPS measurements were carried out by using an Omicron Sphera II hemispherical electron energy analyzer with Monochromatic Al Kα X-ray source (1486.6 eV, anode operating at 15 kV and 300 W). Ar adsorption/desorption isotherm was tested by ASAP 2020 physisorption analyzer (Micromeritics).

Keywords: electrocatalysis · fuel cells · iron · oxygen reduction reaction · sulfur

How to cite: *Angew. Chem. Int. Ed.* **2015**, *54*, 9907–9910
Angew. Chem. **2015**, *127*, 10045–10048

[1] H. A. Gasteiger, S. S. Kocha, B. Sompalli, F. T. Wagner, *Appl. Catal. B* **2005**, *56*, 9.
[2] a) M. Lefevre, E. Proietti, F. Jaouen, J. P. Dodelet, *Science* **2009**, *324*, 71; b) G. Wu, K. L. More, C. M. Johnston, P. Zelenay, *Science* **2011**, *332*, 443; c) W. Ding, Z. D. Wei, S. G. Chen, X. G. Qi, T. Yang, J. S. Hu, D. Wang, L. J. Wan, S. F. Alvi, L. Li, *Angew. Chem. Int. Ed.* **2013**, *52*, 11755; *Angew. Chem.* **2013**, *125*, 11971; d) W. Liang, J. X. Chen, Y. W. Liu, S. L. Chen, *ACS Catal.* **2014**, *4*, 4170.
[3] R. Jasinski, *Nature* **1964**, *201*, 1212.
[4] S. Gupta, D. Tryk, I. Bae, W. Aldred, E. Yeager, *J. Appl. Electrochem.* **1989**, *19*, 19.
[5] a) N. Ramaswamy, U. Tylus, Q. Jia, S. Mukerjee, *J. Am. Chem. Soc.* **2013**, *135*, 15443; b) Y. G. Li, W. Zhou, H. L. Wang, L. M. Xie, Y. Y. Liang, F. Wei, J. C. Idrobo, S. J. Pennycook, H. J. Dai, *Nat. Nanotechnol.* **2012**, *7*, 394.
[6] a) Z. L. Li, G. L. Li, L. H. Jiang, J. L. Li, G. Q. Sun, C. G. Xia, F. W. Li, *Angew. Chem. Int. Ed.* **2015**, *54*, 1494; *Angew. Chem.* **2015**, *127*, 1514; b) H. L. Peng, Z. Y. Mo, S. J. Liao, H. Liang, L. J. Yang, F. Luo, H. Y. Song, Y. L. Zhong, B. Q. Zhang, *Sci. Rep.* **2013**, *3*, 1765; c) F. Jaouen, J. Herranz, M. Lefevre, J. P. Dodelet, U. I. Kramm, I. Herrmann, P. Bogdanoff, J. Maruyama, T. Nagaoka, A. Garsuch, J. R. Dahn, T. Olson, S. Pylypenko, P. Atanassov, E. A. Ustinov, *ACS Appl. Mater. Interfaces* **2009**, *1*, 1623; d) W. H. Niu, X. J. Liu, N. Wang, J. Liu, W. J. Zhou, Z. H. Tang, S. W. Chen, *J. Am. Chem. Soc.* **2015**, *137*, 5555.
[7] E. Proietti, F. Jaouen, M. Lefevre, N. Larouche, J. Tian, J. Herranz, J. P. Dodelet, *Nat. Commun.* **2011**, *2*, 416.
[8] S. W. Yuan, J. L. Shui, L. Grabstanowicz, C. Chen, S. Commet, B. Reprogle, T. Xu, L. P. Yu, D. J. Liu, *Angew. Chem. Int. Ed.* **2013**, *52*, 8349; *Angew. Chem.* **2013**, *125*, 8507.
[9] Q. Wang, Z. Y. Zhou, Y. J. Lai, Y. You, J. G. Liu, X. L. Wu, E. Terefe, C. Chen, L. Song, M. Rauf, N. Tian, S. G. Sun, *J. Am. Chem. Soc.* **2014**, *136*, 10882.
[10] F. Jaouen, E. Proietti, M. Lefevre, R. Chenitz, J.-P. Dodelet, G. Wu, H. T. Chung, C. M. Johnston, P. Zelenay, *Energy Environ. Sci.* **2011**, *4*, 114.
[11] M. B. Ji, Z. D. Wei, S. G. Chen, L. Li, *J. Phys. Chem. C* **2009**, *113*, 765.
[12] C. D. Wagner, L. E. Davis, M. V. Zeller, J. A. Taylor, R. H. Raymond, L. H. Gale, *Surf. Interface Anal.* **1981**, *3*, 211.
[13] a) Y. Z. Su, Y. Zhang, X. D. Zhuang, S. Li, D. Q. Wu, F. Zhang, X. L. Feng, *Carbon* **2013**, *62*, 296; b) J. Liang, Y. Jiao, M. Jaroniec, S. Z. Qiao, *Angew. Chem. Int. Ed.* **2012**, *51*, 11496; *Angew. Chem.* **2012**, *124*, 11664.

Received: April 6, 2015
Revised: May 25, 2015
Published online: July 3, 2015

